Multidye Nanostructured Material for Optical Data Storage and Security Labeling

Ilya Gourevich,† Hung Pham,† James E. N. Jonkman,‡ and Eugenia Kumacheva*,†

Department of Chemistry, University of Toronto, 80 Saint George Street, Toronto, Ontario, M5S 3H6 Canada, and Advanced Optical Microscopy Facility, Ontario Cancer Institute, Princess Margaret Hospital, 610 University Avenue, Toronto, Ontario, M5G 2M9 Canada

Received November 4, 2003. Revised Manuscript Received January 28, 2004

We report the design, synthesis, and application of a multidye polymer nanocomposite with respect to high-density 3D optical data storage and security labeling. Core−shell latex particles containing visible and near-IR dyes in the core-forming polymer and the shell-forming polymer were used as the functional building blocks to produce a multicolored multiphase polymeric material with a minimized energy transfer between the dyes. The core−shell particles were prepared by copolymerizing dye-labeled monomers with the hosting polymer. Data recording was achieved using confocal fluorescent microscopy by selective photobleaching of the dyes periodically distributed in the nanocomposite film.

Introduction

Polymers attract great interest as materials for optical applications. Their ease of functionalization and processing, good performance, and a relatively low cost make them attractive candidates as the components of optical fibers,[1] photoresists,[2] optical limiters,[3] LED,[4] and optical data storage devices.[5]

Polymer composites have been successfully used to enhance material performance or to satisfy multiple functional requirements.[6] Recently, our group has reported the unique properties of a polymer photonic crystal used as a medium for high-density three-dimensional (3D) optical data storage.[7] We used core−shell latex particles with fluorescent cores and optically inert shells to produce a material in which a periodic 3D array of fluorescent domains was embedded in an optically inert matrix.[8] A two-photon confocal microscope was used as a "write−read" head to record bits of information into the material by local photobleaching of the photosensitive domains and, under much lower fluence, read out the resulting pattern. Because of the existence of optically inert zones between the fluorescent domains, the effective optical storage density in the nanostructured periodic material increased by at least a factor of 2 in comparison with a material with a homogeneous structure.[7]

In the present study we increased the number of dyes in the recording medium to achieve a higher storage density: the number of recording modes in binary data storage scales as 2^n where n is the number of photosensitizers that can be individually addressed. Using selective photobleaching of different dyes incorporated in *different* phases of the material, i.e., in the particles and the matrix, we recorded and stored different patterns on the *same* spot of the recording material. A multiphase structure of the polymer limited nonradiative energy transfer between the dyes to a very narrow (ca. 5 nm) region between the phases.[9]

We report the design, synthesis, and application of the multidye polymer nanocomposite with respect to high-density 3D optical data storage and security labeling. We used core−shell latex particles comprising

* To whom correspondence should be addressed. Phone: 416-978-3576. Fax: 416-978-3576. E-mail: ekumache@alchemy.chem.utoronto.ca.
† University of Toronto.
‡ Ontario Cancer Institute.

(1) (a) Zhou, M. *Opt. Eng.* **2002**, *41*, 1631. (b) Nihei, E.; Ishigure, T.; Koike, Y. *Appl. Opt.* **1996**, *35*, 7085. (c) Nihei, E.; Ishigure, T.; Koike, Y. *Appl. Opt.* **1996**, *35*, 2048.

(2) (a) Kim, H. K.; Hove, C.; Ober, C. K. *J. Macromol. Sci., Pure Appl. Chem.* **1992**, *A29*, 787. (b) Gabor, A. H.; Pruette, L. C.; Ober, C. K. *Chem. Mater.* **1996**, *8*, 2282. (c) Bae, Y. C.; Dai, J.; Weibel, G. L.; Ober, C. K. *Polym. Prepr.* **2000**, *41*, 1586. (d) Yu, T.; Ober, C. K.; Kuebler, S. M.; Zhou, W.; Marder, S. R.; Perry, J. W. *Adv. Mater.* **2003**, *15*, 517.

(3) (a) Carlo, S. R.; Shirk, J. S.; Flom, S. R.; Pong, R. G. S.; Ranade, A.; Tai, H.; Baer, E.; Hiltner, A. *Poym. Prepr.* **2002**, 43, 522. (b) Asher, S. A.; Pan, G.; Kesavamoorthy, R. *MCLC S&T, Sect. B: Nonlinear Opt.* **1999**, *21*, 343.

(4) (a) Wohlgenannt, M.; Tandon, K.; Masumdar, S.; Ramasesha, S.; Vardeny, Z. V. *Nature* **2001**, *409*, 494. (b) Wohlgenannt, M.; Jiang, X. M.; Vardeny, Z. V.; Janssen, R. A. J. *Phys. Lett. Rev.* **2002**, *88*, 197401. (c) Hobson, P. A.; Wedge, S.; Wasey, J. A. E.; Sage, I.; Barnes, W. L. *Adv. Mater.* **2002**, *14*, 1393. (d) Zhu, K.; Xie, Z.; Wang, L.; Jing, X.; Wang, F. *J. Polym. Sci., Part A* **2002**, *40*, 1321. (e) Gross, M.; Muller, D. C.; Nothofer, H. G.; Scherf, U.; Neher, D.; Brauchle, C.; Merrholz, K. *Nature* **2000**, *405*, 661.

(5) (a) Natansohn, A.; Rochon, P. *ACS Symp. Ser.* **1997**, *672*, 236. (b) Belfield, K. D.; Schafer, K. J. *Poym. Prepr.* **2002**, *43*, 161. (c) Hagen, R.; Bieringer, T. *Adv. Mater.* **2001**, *13*, 1805. (d) Day, D.; Gu, M.; Smallridge, A. *Adv. Mater.* **2001**, *13*, 1005.

(6) (a) Winiarz, J. G.; Zhang, L.; Lal, M.; Friend, C. S.; Prasad, P. N. *J. Am. Chem. Soc.* **1999**, *121*, 5287. (b) Lin, Y.; Zhang, J.; Brzozowski, L.; Sargent, E. H.; Kumacheva, E. *J. Appl. Phys.* **2002**, *91*, 522. (c) Dunlap, P. N.; Howe, S. E. *Polym. Compos.* **1991**, *12*, 39. (d) Kymakis, E.; Alexandou, I.; Amaratunga, G. A. J. *Synth. Met.* **2002**, *127*, 59.

(7) Siwick, B. J.; Kalinina, O.; Kumacheva, E.; Miller, R. J. D.; Noolandi, J. *J. Appl. Phys.* **2001**, *90*, 5328.

(8) Kumacheva, E.; Kalinina, O.; Lilge, L. *Adv. Mater.* **1999**, *11*, 231.

(9) Feng, J.; Yekta, A.; Winnik, M. A. *Chem. Phys. Lett.* **1996**, *260*, 296.

10.1021/cm030070f CCC: $27.50
Published on Web 03/26/2004

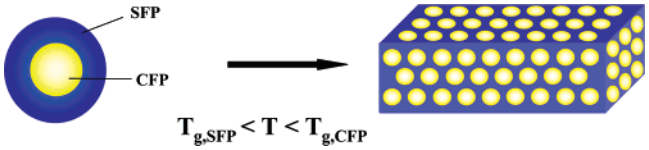

Figure 1. Schematic of the "core−shell" approach to producing multiphase, multidye particles as building blocks for preparation of nanocomposite materials.

visible and near-IR dyes in the different phases as the building blocks of the nanostructured material. Figure 1 shows a schematic of the approach to producing such materials. A core−shell particle contains Dye 1 in the core-forming polymer (CFP) and Dye 2 in the shell-forming polymer (SFP). The specific compositions of the CFP and the SFP provide the relationship $T_{g,SFP} < T_{g,CFP}$ where $T_{g,SFP}$ and $T_{g,CFP}$ are the glass transition temperatures of the SFP and the CFP, respectively. Heat processing of a close-packed periodic array of the core−shell beads under conditions $T_{g,SFP} < T_{annealing} < T_{g,CFP}$ produces a film in which a periodic array of spherical domains containing Dye 1 is incorporated into a matrix containing Dye 2. In principle, this approach can be extended to three- or four-layer particles, resulting in a more complicated morphology and function of the ultimate polymer composite. Selective photobleaching of the two dyes localized on the *same spot* of the polymeric film yields 2^2 storage modes, given that the size of a photoaddressed spot exceeds the size of a microsphere.

The strategy sets several requirements with respect to the properties of dyes and their incorporation into the core−shell particles and the composite material: (i) to avoid cross-talk in the writing and reading processes, the dyes used should have nonoverlapping absorption and emission peaks; (ii) to ensure the localization of dyes in the different phases of the material, diffusion of photoresponsive molecules between the CFP and the SFP has to be suppressed; (iii) the dimensions of the dye-labeled phases in the composite material should be sufficiently large to be spatially resolved with a selected optical technique (for instance, if confocal fluorescence microscopy is chosen for high-resolution writing and reading, the lateral resolution would be $r_{xy} \approx 0.4\lambda_{em}/NA$, where λ_{em} is the emission wavelength and NA is the numerical aperture of the objective lens);[10] (iv) the selected dyes should retain their fluorescent properties during their chemical modification, if covalent attachment of the dyes to the hosting polymer is needed;[11,12] and (v) to simplify the writing and reading processes, it is desirable that the selected dyes all have similar photostabilities.

We chose three dyes for the incorporation in the core−shell particles. Figure 2 shows portions of absorption spectra of the selected dyes. The first dye, 4-chloro-7-nitro-2,1,3-benzoxadiazole (NBD-dye) with absorption peak, λ_{abs}, at 470 nm and emission peak, λ_{em}, at 530 nm was previously used by our group to produce photoactive

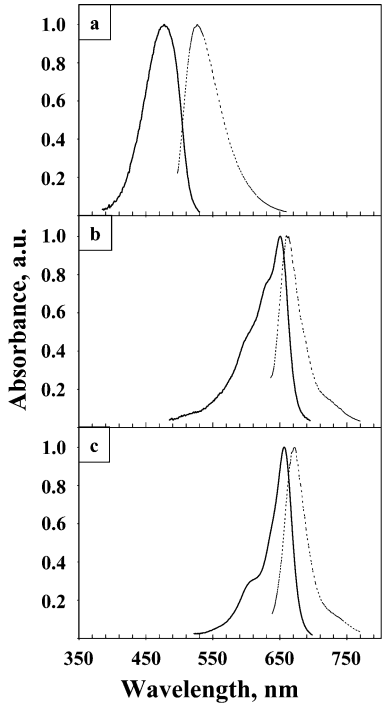

Figure 2. Normalized absorbance (solid line) and fluorescence (dashed line) of NBD (a), Nile Blue (b), and Methylene Blue (c), all dissolved in dichloromethane.

polymer nanocomposites.[7,12,13] Two other dyes had absorption and emission in the near-IR range: 5-amino-9-(diethylamino)-benzophenoxazin-7-ium perchlorate (Nile Blue) with $\lambda_{abs} = 650$ nm and $\lambda_{em} = 665$ nm, and 3,7-bis(dimethylamino)-phenothiazin-5-ium chloride (Methylene Blue) with $\lambda_{abs} = 655$ nm and $\lambda_{em} = 660$ nm. Figure 2 shows portions of absorption and emission spectra of the selected dyes. In the first series of experiments, NBD- and Nile Blue dyes were incorporated into the CFP and the SFP, respectively. In the second series of experiments, CFP was labeled with Methylene Blue whereas the SFP was labeled with NBD.

We demonstrated that the combination of NBD and Nile Blue in the nanostructured polymer material allowed successful selective photobleaching of these dyes and thus ensured multiple writing modes, whereas in the case of Methylene Blue- and NBD-labeled polymers the chemical transformation of Methylene Blue led to weak fluorescence in the composite material in the near-IR-range and hence low efficiency in the reading/writing process.

Experimental Section

Materials. Methyl methacrylate (MMA, 99%), butyl methacrylate (BMA, 99%), ethylene glycol dimethacrylate (EGDMA, 98%), and *tert*-dodecyl mercaptan (t-DDM, 98.5%) were purchased from Aldrich Canada and used without further purification. Water was purified by distillation and then deionized using a Millipore Milli-Q Plus purification system (Millipore Corporation). The ionic initiators, potassium persulfate (KPS, 99%) and ammonium persulfate (APS, 99%), sodium dithionite (85%), sodium carbonate (85%) (all Aldrich Canada), and 2, 2′-azobis(2-methyl-propionitrile) (AIBN, 99%, Kodak) were used as received. Acryloyl chloride (98%) and methacryloyl chloride (98%) (both Aldrich Canada) were distilled before use.

(10) Jonkman J. E. N.; Stelzer, E. H. K. Resolution and Contrast in Confocal and Two-Photon Microscopy. In *Confocal and Two-Photon Microscopy: Foundations, Applications and Advances*; Diaspro, A. Ed.; Wiley-Liss: New York, 2002; p 109.

(11) Generally, covalent attachment leads to a higher optical contrast between the particles and the matrix.

(12) (a) Kalinina, O.; Kumacheva, E. *Chem. Mater.* **2001**, *13*, 35. (b) Kalinina, O.; Kumacheva, E. *Macromolecules* **2002**, *35*, 3675.

(13) Kalinina, O.; Kumacheva, E. *Macromolecules* **2001**, *34*, 6380.

Scheme 1

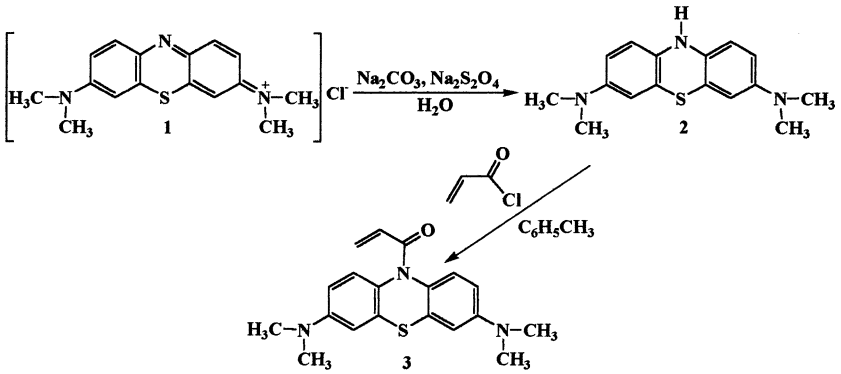

Scheme 2

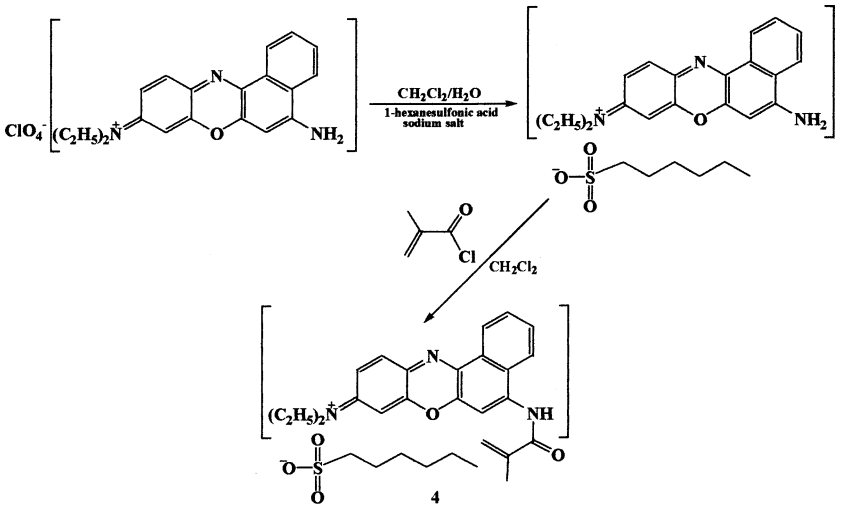

Fluorescent dyes Methylene Blue (MB), Nile Blue (NB), and NBD chloride (all Aldrich Canada) were chemically modified and covalently attached to the corresponding monomer as described below.

Synthesis of Dye-Labeled Monomers. A fluorescent-dye-labeled comonomer 10-acryloyl-*N*,*N*,*N*′,*N*′-tetramethyl-phenothiazine-3,7-diamine (MB-A) was synthesized in two steps (Scheme 1).

Methylene Blue (1.2561 g), 50 mL of water, and 50 mL of toluene were introduced into a two-neck, round-bottom 250-mL flask equipped with a stirring bar under constant nitrogen purge. Then sodium carbonate (1.0 g) and sodium dithionite were added and the resulting mixture was stirred for 30 min at ambient temperature. The aqueous layer was separated, extracted with toluene (3 × 20 mL), and discarded. The combined organic phase was transferred under nitrogen purge into a three-neck, round-bottom flask equipped with a stirring bar and a reflux condenser. Then sodium dithionite (1.0 g) was added and the resulting mixture was heated at reflux temperature until all water was removed. The mixture was cooled to 0 °C and disodium phosphate (2.0 g) and acryloyl chloride (1.23 mL) were added to the flask. The mixture was warmed to the ambient temperature and left overnight under gentle stirring; then it was washed with a 3 wt % disodium phosphate solution (3 × 20 mL), dried over magnesium sulfate, and purified on a silica gel column with ethyl acetate/hexane (1:1) as eluent. The ^{1}H NMR (300 MHz, acetone-d^6) spectrum yielded: δ 7.33 (d, 1H, ^3J = 9.0 Hz, p-H−Ph), 6.74 (d, 1H, ^4J = 2.7 Hz, p-H−Ph), 6.66 (dd, 1H, ^3J = 9.0 Hz, ^4J = 2.7 Hz, o-H−Ph), 6.48 (dd, 1H, $^3J_{trans}$ = 16.8 Hz, $^3J_{cis}$ = 9.9 Hz, =CHCO), 6.32 (dd, 1H, $^3J_{cis}$ = 9.9 Hz, ^2J = 2.4 Hz, CH_2=), 5.64 (dd, 1H, $^3J_{trans}$ = 16.8 Hz, ^2J = 2.4 Hz, CH_2=), 2.94 (s, 12H, $-N(CH_3)_2$). ^{13}C NMR (75 MHz, $CDCl_3$): δ 169.06, 163.97, 148.61, 128.82, 127.89, 127.77, 126.82, 110.49, 110.33, 40.66. GC/MS data: *m*/*z* 339 (M^+), 284 ($M^+ - CH_2$=CHC=O), 268 ($M^+ - CH_2$=CHC=O, $-CH_3$, $-H$), 253 ($M^+ - CH_2$=CHC=O, $-2CH_3$, $-H$), 240 ($M^+ - CH_2$=CHC=O, $-N(CH_3)_2$), 225 ($M^+ - CH_2$=CHC=O, $-N(CH_3)_2$, $-CH_3$), 196 ($M^+ - CH_2$=CHC=O, $-2N(CH_3)_2$).

Scheme 2 shows the synthesis of Nile-Blue-labeled methyl methacrylate (NB-MA). A 1-L Erlenmeyer flask equipped with a magnetic bar was charged with Nile Blue perchlorate (0.9800 g), 1-hexanesulfonic acid sodium salt (3.5246 g), distilled water (250 mL), and dichloromethane (250 mL). The mixture was stirred overnight, and the organic phase was then separated and washed with distilled water (3 × 50 mL). The aqueous phase was combined and extracted with dichloromethane (3 × 50 mL). The combined organic phase was then dried over magnesium sulfate and transferred into a 1-L round-bottom flask equipped with a magnetic bar under constant nitrogen purge. Triethylamine (3.0008 g) was added to the solution under constant stirring. Then methacryloyl chloride (1.5023 g) was added dropwise to the mixture at ambient temperature and the reaction proceeded for 2 h. The solution was then washed with distilled water (3 × 100 mL) and the combined aqueous phase was extracted with dichloromethane (3 × 50 mL). The combined organic phase was dried over magnesium sulfate and purified by flush chromatography with ethyl acetate/dichloromethane mixture (1:1) as eluent. ^{1}H NMR (300 MHz, chloroform-*d*) yielded: δ 8.629 (dd, 1H, ^3J = 8 Hz, ^4J = 1.5 Hz), 8.435 (dd, 1H, ^3J = 8 Hz, ^4J = 1.5 Hz), 7.619 (m, 2H, Hz), 7.546 (d, 1H, ^3J = 9 Hz), 6.614 (dd, 1H, ^3J = 9 Hz, ^4J = 2.7 Hz), 6.371 (d, 1H, ^4J = 2.7 Hz), 6.320 (s, 1H), 6.052 (s, 1H), 5.702 (s, 1H), 3.449 (q, 4H, ^3J = 7 Hz), 2.071 (s, 3H), 1.244 (t, 6H, ^3J = 7 Hz). ^{13}C NMR (75 MHz, $CDCl_3$): δ 156.857, 150.36, 149.208, 146.699, 141.004,140.932, 131.853, 131.443, 130.705, 130.614, 129.854, 127.352, 125.782, 125.493, 124.969, 123.851, 109.222, 100.011, 96.343, 44.99, 18.181, 12.597. ESI MS data: *m*/*z* 386 (M^+).

Table 1. Recipes for Multi-Stage Polymerization of Multidye-Labeled Core−Shell Latex Particles

	MB/NBD		NBD/NB		
	stage 1	stage 2	stage 1	stage 2	stage 3
precharge					
deionized water, g	70	40	70	70	
seeds from previous step, g		20		30	
potassium persulfate, g	0.2				
ammonium persulfate, g			0.2		
AIBN, g		0.001			
pumping mixture					
MMA, g	30.0346	7.4988	30.0403	3.7567	10.0731
BMA, g		7.5194		1.2712	10.0025
EGDMA, g	0.3035	0.1530	0.3153	0.1049	0.3030
Methylene Blue-A, g	0.0128				
Nile Blue-MA					
NBD-MA, g		0.006	0.0347		
t-DDM, g	0.09	0.0495	0.0973	0.0108	0.0513
AIBN, g		0.012		0.0519	0.1025
ionic initiator solution					
water, g		50			10.31
potassium persulfate, g		0.005			
ammonium persulfate, g					0.2451
particle size, nm	590	920	570		1064

Scheme 3

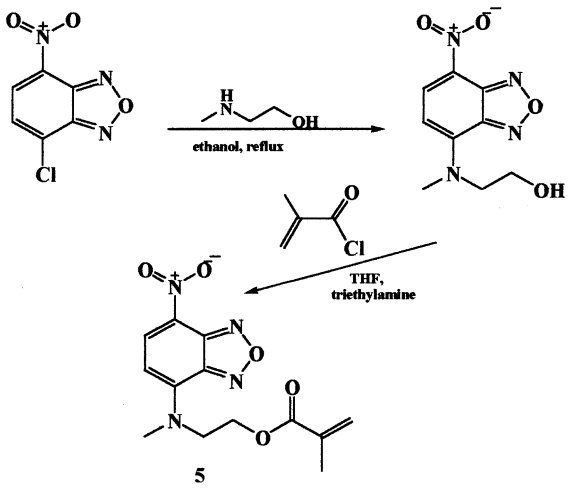

NBD-labeled comonomer (2-methyl-(7-nitro-2, 1, 3-benzoxadiazol-4-ylamino)ethyl-2-methyl methacrylate (NBD-MA) (**5**) was prepared using Scheme 3, as described elsewhere.[14]

Latex Synthesis. We prepared two types of core−shell dye-labeled latex particles. In the first system, the CFP was labeled with NBD-dye (λ_{abs} = 470 nm) and the SFP contained NB-dye absorbing at λ_{abs} = 580 nm. In the second system, the CFP contained MB-dye (λ_{abs} = 650 nm) and the SFP was labeled with NBD-dye. All core−shell latex particles were synthesized using a multistage surfactant-free emulsion polymerization. The reactions were carried out at 80 ± 0.1 °C under positive nitrogen pressure in a three-neck flask equipped with a reflux condenser, a nitrogen inlet, and a mechanical stirrer.

Synthesis of Latex Particles with MB-Labeled Cores and NBD-Labeled Shells. *Stage 1: Synthesis of Latex Particles with MB-Labeled Cores.* The reactor was charged with water and KPS or APS and then it was purged with nitrogen for 30 min. Then a mixture of MMA and MB-A, a chain transfer agent (t-DDM), and a cross-linking agent (EGDMA) were introduced into the reactor using a fluid-metering pump. The feeding time was usually 3−4 h. After feeding was complete, the reaction was continued for 1 h.

Stage 2: Synthesis of NBD-Labeled Shells. Latex dispersion (ca. 20 g) from Stage 1, water, and a small portion of AIBN were mixed in the reaction flask. Then a mixture of MMA and BMA, a fluorescent comonomer NBD-MA, AIBN, EGDMA, and t-DDM was introduced into the reactor at a rate of 0.09 mL/min. A water solution of an anionic initiator KPS was added simultaneously with the monomer mixture using a different fluid-metering pump.

Synthesis of Latex Particles with NBD -Labeled Cores and MB-Labeled Shells. *Stage 1: Synthesis of NBD-Labeled Cores.* This stage was similar to Stage 1 in the synthesis of latex particles with MB-labeled cores (see above) but instead of MB-A a dye-labeled monomer NBD-MA was introduced into the reactor.

Stage 2: Synthesis of Intermediate Optically Inert Shell. Latex dispersion (ca. 30 g) from Stage 1 and a DI water were mixed in the reaction vessel. A mixture of MMA and BMA in weight ratio 3:1, AIBN, EGDMA, and t-DDM were fed into the reactor at a rate of 0.09 mL/min.

Stage 3: Synthesis of NB-Labeled Shell. A mixture of MMA and BMA (weight ratio 1:1), AIBN, fluorescent comonomer NB-MA, EGDMA, and t-DDM was fed into the reactor at a rate of 0.09 mL/min. A water solution of anionic initiator APS was added simultaneously with a monomer mixture using a separate fluid-metering pump.

The recipes for the synthesis of the dye-labeled core−shell particles are given in Table 1.

Latex Characterization. The dimensions and the size distribution of latex particles were examined by scanning electron microscopy (SEM) using a Hitachi S-570 scanning electron microscope at an accelerating voltage of 15 kV and a working distance of 10 mm. A droplet of a dilute latex dispersion was dried on an aluminum stub and then gold-coated. The polydispersity index (PDI) of the particles was obtained by image analysis of the SEM micrographs.

Preparation of Polymer Films. Latex dispersions were poured into a funnel with a 0.45-μm PTFE filter at the bottom, which was then covered with a glass slide to suppress water evaporation. When the particles settled, a clear supernatant liquid was carefully removed, and the remaining water was allowed to evaporate from the particle sediment. The dry sediments were heat processed at 120 °C for 15 ± 1 h.

Studies of Film Morphology. The surface and the bulk morphologies of the polymer films were studied using a Zeiss 510 upright confocal microscope equipped with an argon-ion laser (wavelengths 458 and 488 nm) and a helium neon laser (wavelength 633 nm). A 488-nm line of the Ar-ion laser was used for the excitation of the NBD-dye. Methylene blue and Nile Blue were excited using λ_{ex} = 633 nm. The lateral resolution was about 0.2 and 0.3 μm for the NBD and near-IR dyes, respectively, and the pinholes were adjusted to give an optical section of about 1.0 μm for all dyes. A high-resolution

(14) (a) Kalinina, O.; Kumacheva, E. *Macromolecules* **1999**, *32*, 4122. (b) Sosnowski, S.; Feng, J.; Winnik, M. A. *J. Polym. Sci., Part A: Polym. Chem.* **1994**, *32*, 1497.

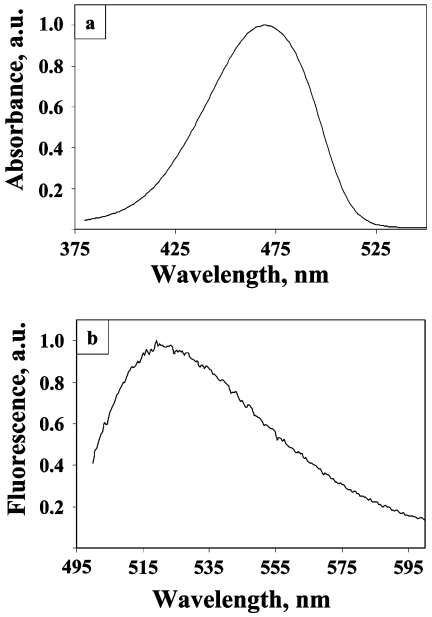

Figure 3. Normalized absorbance (a) and fluorescence (b) of NBD-labeled PMMA in tetrahydrofurane (THF) solution; $\lambda_{exc} = 488$ nm.

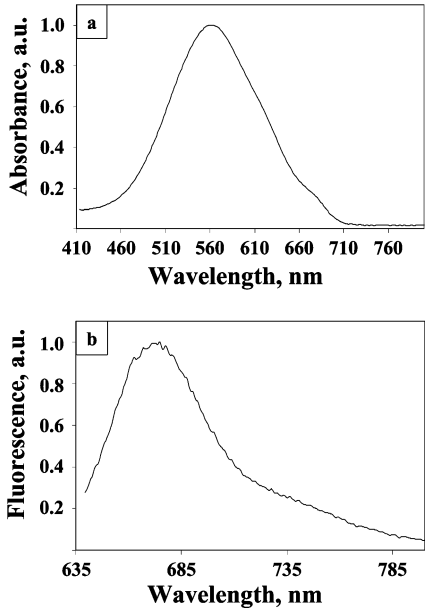

Figure 4. Normalized absorbance (a) and fluorescence (b) of Nile-Blue-labeled PMMA in THF solution; $\lambda_{exc} = 633$ nm.

oil immersion lens (100×/1.4 NA) with a working distance of 0.1 mm was used.

Information Recording and Readout. Typically, the writing intensities were at least 100 times greater than the reading intensities. We used 20 scans ($\lambda_{ex} = 458$ nm) of Argon-ion laser at 6.25 mW to record patterns in the NBD-labeled polymer. The 488-nm line of the argon-ion laser with laser power 0.03 mW and with 4 averaging scans was used to "read" the recorded pattern.

The 633-nm line of the HeNe laser with laser power 5 mW and 500 scans were used for encoding information in MB- and NB-labeled polymers. The same line was used for "reading" the patterns with 4 averaging scans at laser power 5 and 0.025 mW, respectively.

Results

NBD-Labeled Polymer. Figure 3a and b show portions of absorption and emission spectra, respectively, for NBD-labeled PMMA. Comparison of these spectra with Figure 2a shows that modification and subsequent copolymerization of NBD-MA with MMA does not significantly change the absorption and emission peaks for the unmodified dye.

Nile Blue-Labeled Polymer. Figure 4a and b show portions of absorption and emission spectra, respectively, for NB-labeled PMMA-*co*-PBMA. A significant broadening of absorption peak occurred in comparison with the nonmodified dye (Figure 2b); in addition, the position of absorption maximum was blue-shifted from 650 to 560 nm. We ascribe the changes in the spectrum to a high sensitivity of Nile Blue to the chemical environment.[15] In addition, during the modification of Nile Blue the attachment of the electron-withdrawing group to the nitrogen atom caused redistribution of electron density in the molecule.[16] In Figure 4b the emission maximum of NB-labeled PMMA-*co*-PBMA only slightly red-shifted from 665 to 675 nm, in comparison with Figure 2b.

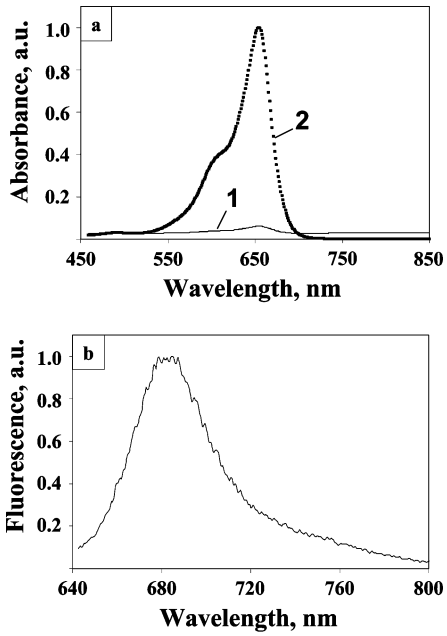

Figure 5. (a) Normalized absorbance of leuco-Methylene-Blue (spectrum 1) and Methylene-Blue-labeled PMMA (spectrum 2); (b) normalized fluorescence of Methylene-Blue-labeled PMMA excited at 633 nm. All samples were dissolved in THF.

Methylene Blue-Labeled Polymer. Figure 5a shows portions of absorption spectra of Methylene Blue in the leuco-form (product 3, Scheme 1) and the MB-labeled PMMA. In a comparison of the absorption spectra in Figure 2c and in Figure 5a, spectrum 1 indicates that in the leuco-form MB shows no absorption in the spectral range from 550 to 670 nm. The absence of an absorption peak for leuco-MB is due to the reduction in conjugation length in the modified molecule, caused by a transition from a planar structure of the dye to a nonplanar structure of the molecule in the leuco-form.[17] An absorption peak with a maximum at 650 nm appeared again in the spectrum of MB-labeled PMMA

(15) Krihak, M.; Murtagh, M. T.; Shahriari, M. R. *J. Sol-Gel Sci. Technol.* **1997**, *10*, 153.
(16) (a) Hutchings, M. G. *Tetrahedron* **198**4, *40*, 2061. (b) Hallas, G.; Towns, A. D. *Dyes Pigm.* **1997**, *33*, 205.

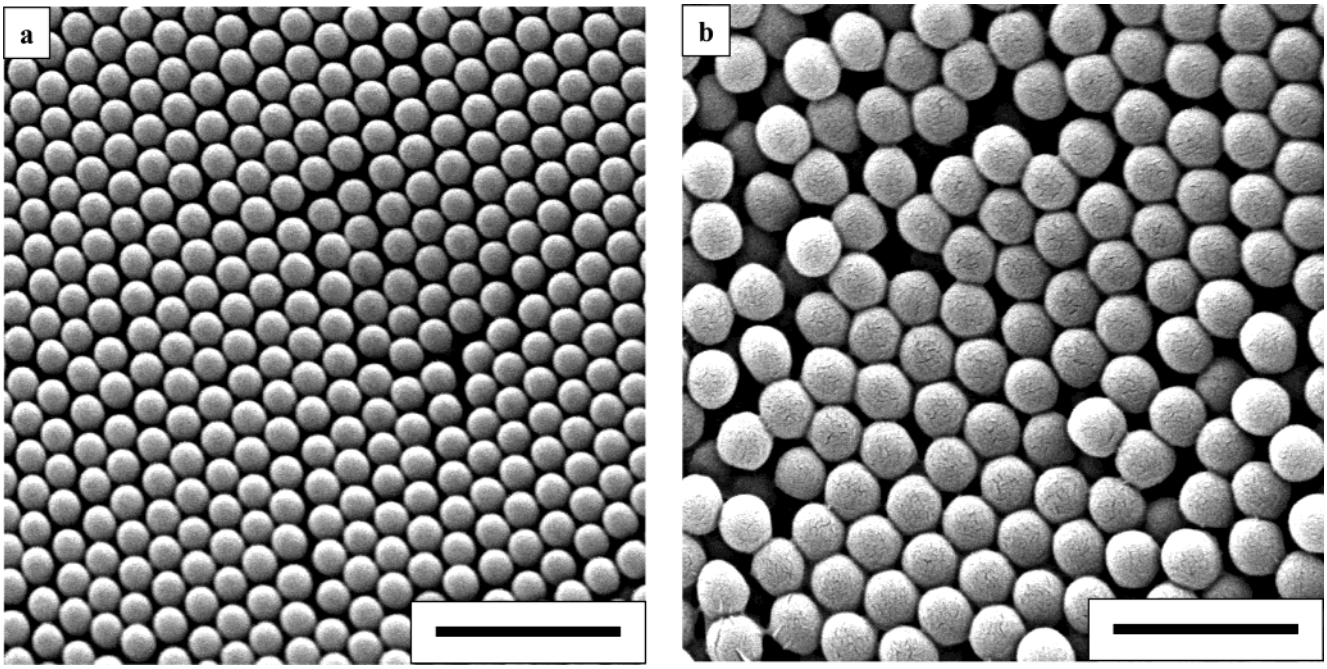

Figure 6. SEM image of Methylene-Blue-labeled PMMA core particles (a), and core−shell particles with Methylene-Blue-labeled PMMA cores and PMMA-*co*-PBMA NBD-labeled shells (b). Scale bar is 3.0 μm.

(Figure 5a, spectrum 2). This effect originated from the photoinduced oxidation of product 3, followed by the loss of acrylic moiety, which restored the planarity of the molecular structure of MB.[18] All above transformations were accompanied by a change in color of the system: a freshly prepared solution of leuco-Methylene Blue was pale yellow, after 4 h exposure to ambient light it became green, and after 24 h it turned into dark blue.

Figure 5b shows strong emission of MB-labeled PMMA with a maximum at 680 nm. The position of the emission peak is close to that measured for the Methylene Blue dye (Figure 2c).

We note that absorption at 470 nm and emission at 530 nm make NBD a complementary couple for near-IR dyes: the absorption maxima are sufficiently far which allows selective excitation of the two dyes during recording and readout processes.

Synthesis of Multicolored Core−Shell Particles. The core−shell latex particles with MB-labeled 590-nm-size cores and NBD-labeled 175-nm-thick shells were prepared using the recipes given in Table 1. The MB-labeled monodisperse PMMA cores (PDI < 1.03) were synthesized in Stage 1. These particles were cross-linked with 1 wt % of EGDMA to suppress diffusion of the dye-labeled polymer chains between the CFP and the SFP. In Stage 2, NBD-labeled PMMA/PMMA-*co*-PBMA shell was polymerized on the surface of the MB-labeled cores. Figure 6a and b show typical SEM images of the MB-labeled cores and the core−shell particles, respectively.

The core−shell particles with NBD-labeled cores and NB-labeled shells were synthesized using a modified approach. The probability of nonradiative energy transfer is higher for the NBD/NB pair than for the NBD/MB pair because, in comparison with MB, absorption of NB is substantially broader and is blue-shifted (Figures 4a and 5a, respectively). To reduce intimate contact between the NBD- and Nile-Blue-labeled phases in addition to cross-linking of the NBD-labeled CFP we synthesized an intermediate optically inert 20-nm-thick shell on the surface of the NBD-PMMA core. This shell also suppressed diffusion of the low-molecular-weight dye-labeled polymer chains between the neighboring compartments of the core−shell particles. The SEM images of the NBD-labeled particles and the NBD/NB-labeled core−shell beads were similar to those of MB/NBD shown in Figure 6a and b, respectively.

Following particle sedimentation, dry sediments were heat processed at 120 °C, yielding transparent polymeric films. The morphology of these films examined with confocal fluorescent microscopy depended on the excitation wavelength used for imaging.

Figure 7a and b show the morphology of films comprising the NBD and Nile Blue dyes. When λ_{exc} = 633 nm was used for dye excitation, only Nile Blue localized in the polymer matrix (i.e., the SFP) was excited, while the NBD-dye localized in the CFP remained optically inactive. Under these conditions, the structure of the film appeared as a periodic array of black spots on the bright background of the NB-labeled matrix (Figure 7a). An inverse structure was observed when the 488-nm line of the Ar-ion laser was used to excite the NBD-dye localized in the PMMA cores. Figure 7b shows a periodic array of bright domains on the dark background of the NB-labeled matrix.

In the second stage, the composite films containing NBD and NB were used as the recording medium. To record patterns in the composite material, we used selective photobleaching to quench fluorescence of a particular dye leaving the second dye unaffected. The same confocal microscope was used as the writing/

(17) (a) Jones, G.; Yan, D. X.; Gosztola, D. J.; Greenfield, S. R.; Wasielewski, M. R. *J. Am. Chem. Soc.* **1999**, *121*, 11016. (b) Lezna, R. O.; de Tacconi, N. R.; Hahn, F.; Arvia, R. J. *J. Electroanal. Chem.* **1991**, *306*, 259.

(18) Hallock, A. J.; Berman, E. S. F.; Zare, R. N. *J. Am. Chem. Soc.* **2003**, *125*, 1158.

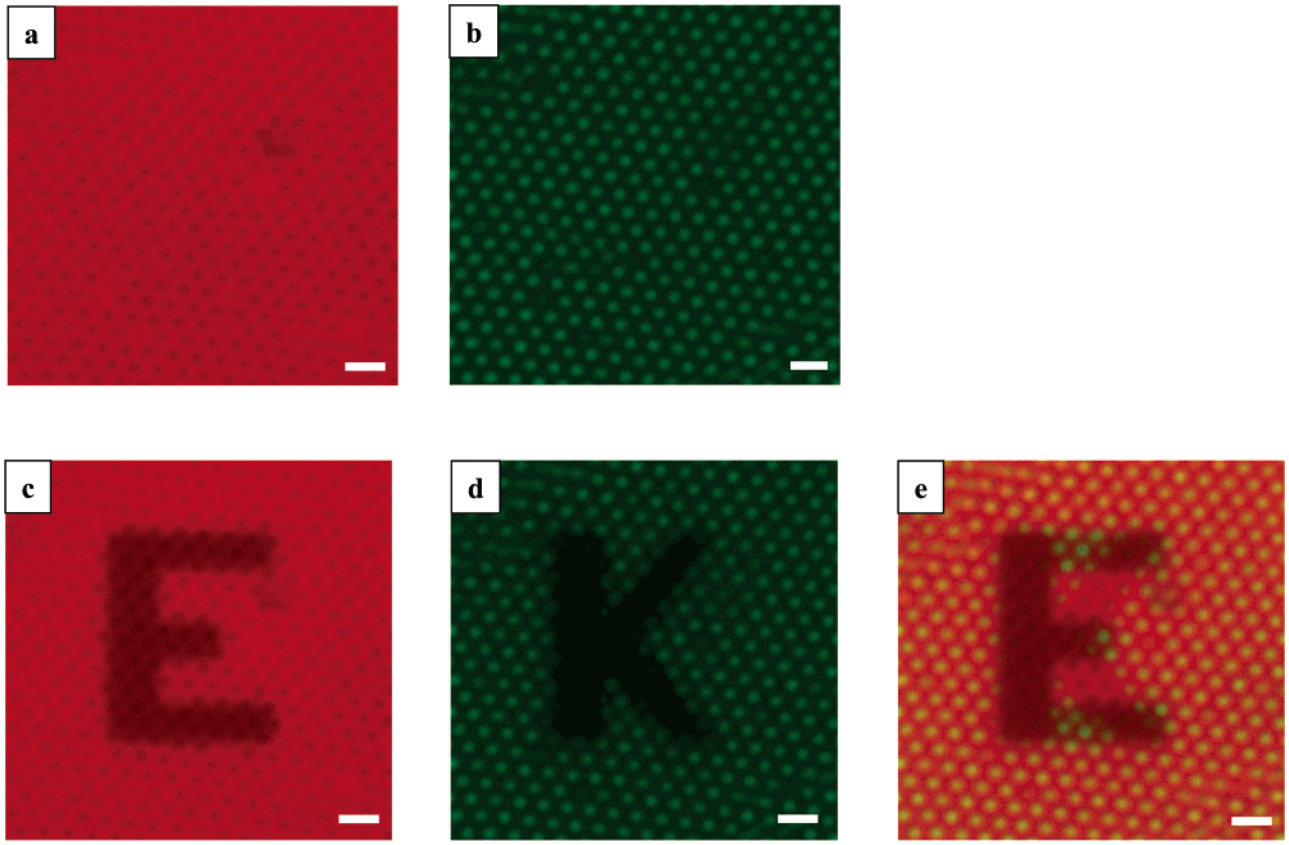

Figure 7. Confocal images of the multidye multiphase polymeric films: (a) Nile-Blue-labeled PMMA-*co*-PBMA matrix (λ_{exc} = 633 nm); (b) NBD-labeled PMMA particles (λ_{exc} = 488 nm); (c) letter "E" photobleached in the Nile-Blue-labeled matrix (λ_{exc} = 633 nm); (d) letter "K" photobleached in the NBD-labeled polymer (λ_{exc} = 458 nm); and (e) superimposed images c and d. Scale bar is 2 μm. The addressed plane is localized 6.0 μm below the film surface.

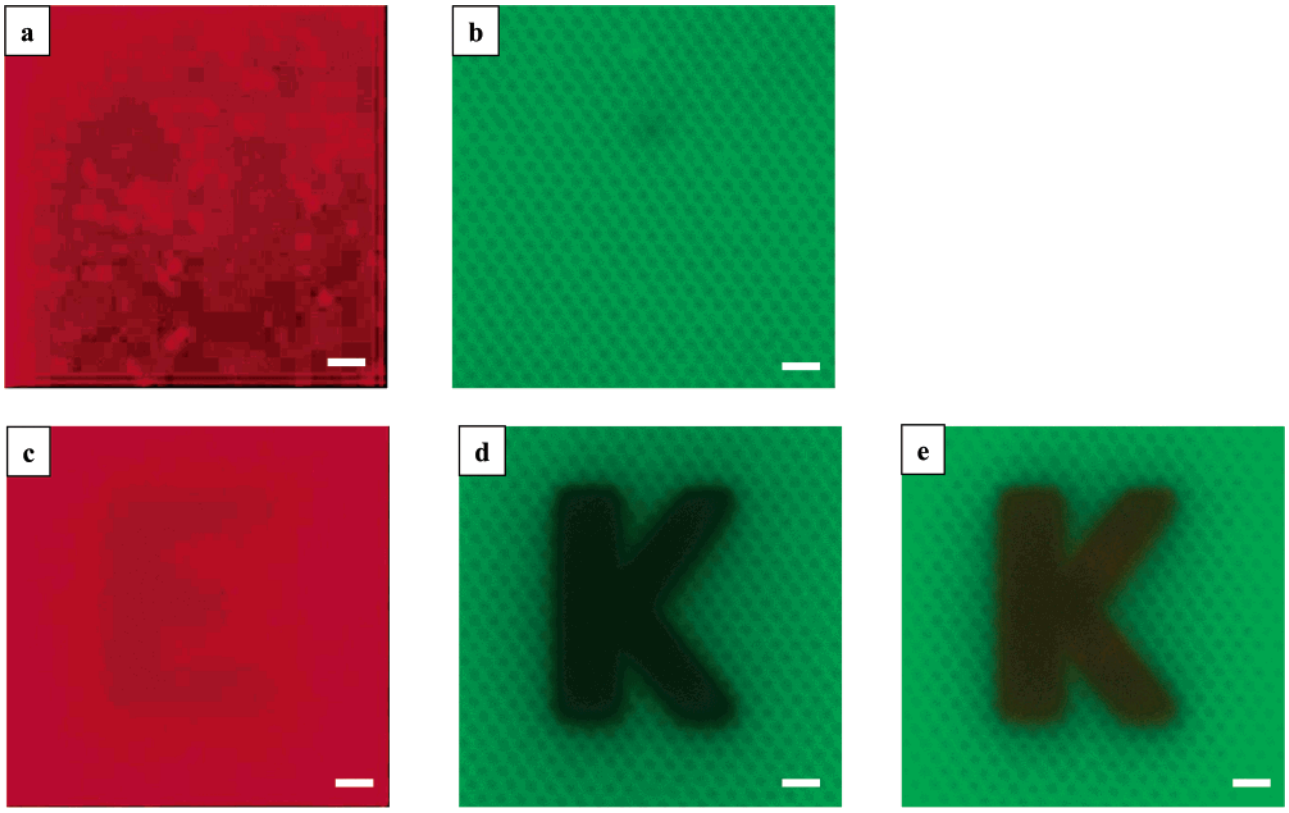

Figure 8. Confocal images of the multidye multiphase polymeric films: (a) Methylene-Blue-labeled PMMA particles (λ_{exc} = 633 nm); (b) NBD-labeled PMMA-*co*-PBMA matrix (λ_{exc} = 488 nm); (c) letter "E" photobleached in the Methylene-Blue-labeled PMMA particles (λ_{exc} = 633 nm); (d) letter "K" photobleached in the NBD-labeled PMMA-*co*-PBMA matrix (λ_{exc} = 488 nm); and (e) superimposed images c and d. Scale bar is 2 μm. The addressed plane is localized 6.0 μm below the film surface.

reading head. The letter "E" was written by photobleaching Nile Blue using $\lambda_{exc} = 633$ nm (Figure 7c). The letter "K" (Figure 7d) was written on the *same* spot byphotobleaching NBD using $\lambda = 458$ nm.[19] Readout was accomplished at a reduced laser power. Figure 7e shows a combined readout of the two letters. Except for the areas of spatial overlap, no cross-talk appeared between the letters.

Figure 8 shows the structure of the polymer films comprising Methylene Blue and NBD. When Methylene Blue was excited with $\lambda_{exc} = 633$ nm only a weak fluorescent signal was observed and the imaged plane did not feature a characteristic periodic pattern (Figure 8a). However, when NBD localized in the matrix phase was excited with $\lambda = 488$ nm a characteristic "inverse" structure with bright background and dark periodic dots was observed (Figure 8b).

Figure 8d and e show the results of recording and reading experiments in the MB/NBD polymer films. We attempted to write the letter "E" by photobleaching MB-labeled core-particles ($\lambda_{exc} = 633$ nm) and then read it out at reduced laser power at $\lambda_{exc} = 633$ nm (Figure 8c). As expected, photobleaching of MB did not produce a pattern in the film. Then, using $\lambda_{exc} = 488$ nm the letter "K" was written by photobleaching NBD incorporated into the matrix phase (Figure 8d). The combined image in Figure 8e shows only letter "K", not notably affected by the irradiation with a $\lambda = 633$ nm.

Discussion

The absence of cross-talk in the writing/reading process shows the feasibility of selective photobleaching of several dyes as a tool for multiple writing on the same spot of a photoresponsive material. Our results demonstrate that multidye multiphase films can be successfully used for high-density 3D optical data storage and security writing. In the first application, further increase in storage capacity can be achieved by reducing the size of the recorded pattern (yet, keeping it larger than the size of a single core−shell particle) and by enhancing depth discrimination via two-photon dye excitation and photobleaching.[20] Information can be recorded pixel by pixel as a binary code for high-resolution recording by addressing one or two dyes. For security writing, recording can be accomplished by recording the pattern through a mask or using a scanning technique as used in the current work.

Although the photobleaching process likely involves photooxidation, little is known about the detailed reaction mechanisms, which may be different for each of the dyes we used. This difference results in a different photostability of the dyes, important in the writing process: for instance, in comparison with NBD, photobleaching of NB required a great increase in the number of scans and thus increase in recording time. We note that in the compromise between the long recording time and high photostability of the dyes, the latter feature is more important because it reduces destructive readout of the pattern.[21] Comparison of film structures in Figures 7a and c and 8a and c proves the importance of covalent attachment of the dyes to the hosting polymer, and, in general, underlines the requirements to the selected dyes. Whereas NB-dye retained its fluorescent properties after modification, covalent attachment to the monomer and the incorporation into the polymer, MB underwent several chemical transformations. First, leuco-Methylene Blue obtained after its chemical modification was not fluorescent. During latex synthesis and/or film preparation fluorescent Methylene Blue formed again as a result of photooxidation of the leuco-dye.[22] These transformations had several consequences. First, the amount of Methylene Blue produced in-situ was insufficient to provide strong fluorescence. Second, the low-molecular dye diffused between the particles and the matrix, i.e., between the CFP and the SFP, reducing optical contrast in the film. In addition, partial segregation of MB produced irregular bright domains, shown in Figure 8a.

Finally, to provide sufficient signal-to-noise ratio in the readout process, dye photobleaching should result in at least 20% reduction in fluorescence intensity of the dyes. In our work, however, we reduced fluorescence intensity by ca. 60%, which increased the recording time.

Summary

We synthesized core−shell latex particles with cores and shells labeled with visible and near-IR fluorescent dyes. These particles were used for the preparation of a multidye polymer nanocomposite material with potential applications in high-density 3D optical data storage and security labeling. *Different* patterns were recorded on the *same* spot of the composite material using selective photobleaching of the dyes localized in different phases of the material. We also demonstrated the importance of covalent attachment of dyes to the hosting polymers as the means to prevent their aggregation and diffusion between the different phases.

CM030070F

(19) The 458-nm band was used for encoding information in ordered domains of PMMA beads to avoid simultaneous bleaching of Nile blue during "writing", which occurred when high power 488-nm band was used.

(20) In the current work, one-photon-induced photobleaching provided depth discrimination of about 15 μm.

(21) Some dyes succumb to decomposition during the polymerization process. Thus, a proper adjustment should be made to control effective dye concentration in the host polymer.

(22) Gensler, W. J.; Jones, J. R.; Rein, R.; Bruno, J. J.; Bryan, D. M. *J. Org. Chem.* **1966**, *31*, 2324.